Pergamon

Bioorganic & Medicinal Chemistry 10 (2002) 3731–3739

BIOORGANIC & MEDICINAL CHEMISTRY

Design, Synthesis, Conformational Analysis, and Biological Studies of Urotensin-II Lactam Analogues

Paolo Grieco,[a] Alfonso Carotenuto,[b] Riccardo Patacchini,[c] Carlo A. Maggi,[c] Ettore Novellino[a] and Paolo Rovero[b,*]

[a]*Department of Pharmaceutical and Toxicological Chemistry, University of Naples 'Federico II', I-80131 Naples, Italy*
[b]*Department of Pharmaceutical Sciences, University of Salerno, I-84084 Fisciano, Italy*
[c]*Department of Pharmacology, Menarini Ricerche SpA, I-50131 Florence, Italy*

Received 3 May 2002; accepted 9 August 2002

Abstract—Human urotensin II (hU-II; H-Glu-Thr-Pro-Asp-cyclo[Cys-Phe-Trp-Lys-Tyr-Cys]-Val-OH) is a disulfide bridged undecapeptide recently identified as the ligand of an orphan G protein-coupled receptor. hU-II has been described as the most potent vasoconstrictor compound identified to date. With the aim of replacing the disulfide bridge by a chemically more stable moiety, we have synthesized and tested a series of lactam analogues of hU-II minimum active fragment, that is hU-II(4–11). The contractile activity of the synthetic analogues on the rat isolated thoracic aorta was found to be dependent upon the dimension of the lactam bridge. The most active peptide, H-Asp-cyclo[Orn-Phe-Trp-Lys-Tyr-Asp]-Val-OH (**3**), is approximately 2 logs less potent than hU-II ($pD_2 = 6.3$ vs 8.4). A conformational analysis in solution of the active peptide **3**, one of the inactive analogues, and hU-II was performed, using NMR and molecular modelling techniques. A superposition of the calculated structures of hU-II and **3** clearly shows that three out of four key residues (i.e., Phe^6, Lys^8 and Tyr^9) maintain the same side– chain orientation, while the fourth one, Trp^7, cannot be superimposed. This observation could explain the reduced biological activity of the synthetic analogue.

Introduction

Urotensin II is a cyclic peptide originally isolated from the urophysis, the hormone storage-secretion organ of the caudal neurosecretory system of teleost fishes, and sequenced more than 20 years ago.[1] Several structural forms of U-II have subsequently been reported in different species of fish and amphibians, with variation occurring in the five to seven N-terminal residues, followed by a C-terminal conserved, disulfide bridged cyclic hexapeptide (Fig. 1). These peptides showed general smooth muscle contracting activity in fish[2] and goby U-II additionally possesses vasoconstrictor activity in rats.[3] Recently, urotensin-II was cloned in several mammalian species, including humans.[4] Human U-II (hU-II) is an 11 amino acid peptide that retains the cyclic portion typical of fish U-II (Fig. 1).

In 1999 Ames et al.[5] identified a new human G-protein coupled receptor homologous to the GPR14/SENR orphan receptor from rat.[6] The use of a 'reverse molecular pharmacology' approach[7] identified U-II as the ligand of this orphan receptor. Interestingly, three other independent groups reported similar results within 2 months.[8] As a result, there has been continued interest in U-II sequences and several reports have described hU-II to be a very potent constrictor of certain human isolated arteries and veins[9] as well as of several vessels from different mammalian species.[10] hU-II has been shown to be one to two orders of magnitude more potent than endothelin-1 in producing vasoconstriction in mammals and thus is one of the most effective vasoconstrictor compounds identified to date.[5,11] Moreover, hU-II produces contractions in a number of non-vascular smooth muscle tissues, such as primate airways[12] and human heart.[13] Interestingly, no differences were noted between the effects produced by human and rat isoforms of urotensin-II[14] indicating that the conserved cyclohexapeptide sequence is mainly responsible for biological activity. Both hU-II immunoreactivity and receptors for hU-II have been identified in human cardiac tissues[5,9b] and hU-II has been shown to produce very potent inotropic effects in human atrium and ventricle.[13]

*Corresponding author. Tel.: +39-089-962809; fax: +39-089-962828; e-mail: rovero@unisa.it

0968-0896/02/$ - see front matter © 2002 Elsevier Science Ltd. All rights reserved.
PII: S0968-0896(02)00372-3

H-Glu-Thr-Pro-Asp-[**Cys-Phe-Trp-Lys-Tyr-Cys**]-Val-OH	Human (hU-II)
H-Ala-Gly-Thr-Ala-Asp-[**Cys-Phe-Trp-Lys-Tyr-Cys**]-Val-OH	Goby
H-Gly-Pro-Thr-Ser-Glu-[**Cys-Phe-Trp-Lys-Tyr-Cys**]-Val-OH	Pig
H-Gln-His-Gly-Ala-Ala-Pro-Glu-[**Cys-Phe-Trp-Lys-Tyr-Cys**]-Val-OH	Mouse
H-Gln-His-Gly-Thr-Ala-Pro-Glu-[**Cys-Phe-Trp-Lys-Tyr-Cys**]-Val-OH	Rat

Figure 1. Amino acid sequences of U-II isopeptides from different species.

Therefore, this peptide may be associated to the maintenance of cardiovascular homeostasis in man. Unfortunately, as the biological studies on hU-II progress, limited structure–activity relationship is available to provide information on the residues responsible for the activity of this sequence.[15] Additionally, hU-II synthetic analogues acting as agonists or antagonists would be extremely important tools for exploring the (patho)-physiological role of this peptide. Accordingly, in this study we have investigated the synthesis, the conformational properties, and the biological activities of cyclic lactam analogues of U-II C-terminal portion. As biological assay we chose the rat isolated thoracic aorta, a preparation that has been reported to be the most sensitive and reliable one over a broad range of human and nonhuman vessels, for evaluating biological activities of hU-II and related peptides.[16] Since the conserved C-terminal cyclic portion of U-II was considered a valuable starting point,[3,17] replacement of the disulfide bridge by a chemically more stable moiety appeared as an attractive alternative.

The replacement of a disulfide bridge by a side chain-to-side chain lactam bridge has been previously reported in several biologically relevant peptides, such as conotoxins,[18] endothelin-1,[19] HIV gp41 antigenic loop,[20] and a somatostatin analogue.[21] In all of these examples, the biological activity was retained or increased compared to the unmodified sequence. In the somatostatin analogue case, a sequence structurally and biologically related to U-II, the biological activity was strongly dependent upon the size of the lactam bridge. Accordingly, we will present a correlation between ring size and biologically activity for U-II analogues.

Results

Design and synthesis

As a starting structure for this study, we selected the minimum active fragment of hU-II, that is hU-II(4–11),[3,17] which also represents the portion of the molecule conserved among the different isopeptides that has been previously described (Fig. 1). The Cys residues in positions 5 and 10 were replaced by amino acids bearing an amino ((2,3)-diaminopropionic acid (Dap), ornithine (Orn) or lysine (Lys)) and carboxylic (Asp or Glu) functions on the side chain, respectively; these two side chains were subsequently linked to form the key lactam bridge. Accordingly, we were able to modulate the dimension of the cycle from a minimum of 20 atoms (Dap-Asp; peptide no. **1** in Table 1) to a maximum of 24 atoms (Lys-Glu; peptide no. **5**).

The peptides were constructed by standard 9-fluorenylmethoxycarbonyl (Fmoc) chemistry using an appropriate orthogonal protection strategy. Couplings were carried out with in situ activating reagents routinely used in Fmoc solid–phase peptide synthesis (SPPS), such as an *N*-hydroxybenzotriazole (HOBt)-based uronium salt 2-(1*H*-benzotriazole-1-yl)-1,1,3,3-tetramethyluronium hexafluorophosphate (HBTU) in the presence of a tertiary base *N,N*-diisopropylethylamine (DIPEA). The lactam bridge was obtained using the Allyl and allyloxycarbonyl (Alloc) protection strategy as previously reported.[22] Peptides were released from the solid support using a cleavage cocktail of 90% trifluoroacetic acid (TFA), 5% water, and 5% Et_3SiH. The addition of a trialkylsilane to a cleavage mixture reduces the amount of alkylation of the Trp residues with the cations generated during cleavage.[23] The HPLC profiles of the crude peptides following cleavage showed one major peak corresponding to the cyclic peptide along with a small quantity of the linear peptide as a contaminant. The peptides were purified by preparative reversed-phase high–performance liquid chromatography (RP-HPLC) and the purity and physicochemical properties of the purified peptides assessed by MS and HPLC (see Table 2).

Pharmacology

hU-II (0.1–100 nM) produced slowly-developing, sustained and concentration-dependent contractile responses averaging 76±7% of maximal contraction from KCl at 80 mM. The potency of hU-II calculated in our experiments ($pD_2 = 8.4$; Table 1) was comparable to that reported by Ames and coworkers ($pD_2 = 9.09$)[5] for the same bioassay. For the five hU-II analogues tested in our study, only one sequence (**3**) maintained full agonist activity; a maximal response averaging 90±5% (at 30 μM; $n = 4$) of that produced by hU-II. The potency in eliciting contractile responses of **3** was about 100-fold lower than hU-II ($pD_2 = 6.3$ vs 8.4, respectively). Peptide **1** produced contractile responses only at μM concentrations. At 30 μM, which was the highest concentration examined, **1** produced a response averaging 48±1% ($n = 4$) to hU-II, a potency more than three orders of magnitude lower than the latter. The

Table 1. Structure and contractile activity of U-II lactam analogues on the rat isolated thoracic aorta
General formula: H-Asp-cyclo[Xaa-Phe-Trp-Lys-Tyr-Yaa]-Val-OH

Peptide	Xaa	Yaa	n[a]	pD_2 [b]
U-II	Cys	Cys	20	8.4 ± 0.1
1	Dap	Asp	20	≤ 4.5
2	Dap	Glu	21	n.a.[c]
3	Orn	Asp	22	6.3 ± 0.3
4	Lys	Asp	23	n.a.
5	Lys	Glu	24	n.a.

[a]n, number of atoms engaged in the cycle.
[b]pD_2, $-\log EC_{50}$.
[c]n.a., no activity up to 30 μM. Each value in the table is mean ± SEM of at least four determinations.

remaining three compounds were inactive as agonists at concentrations as high as 30 μM. In the presence of **2**, **4** or **5** (30 μM each), hU-II (10 nM) produced a contractile response comparable to that obtained in the untreated preparation controls. This data eliminates the potential for these compounds to act as an antagonist at the hU-II receptor.

NMR and molecular modeling analysis

Nuclear Magnetic Resonance (NMR) and molecular modeling techniques were used to study the solution structure of hU-II, **2**, and **3**. The latter was chosen since it is the most active compound, while **2** was selected among the inactive peptides. We recorded NMR spectra in dimethylsulfoxide (DMSO)-d_6, which is a typical structure stabilizing solvent, acting by favoring the intramolecular hydrogen bonds and, consequently, folded conformations. In addition, the use of viscous solvent medium can affect the equilibrium among isoenergetic conformers, selecting the more ordered conformers.[24] NMR analysis was performed using one dimensional (1D) and two-dimensional (2D) proton homonuclear techniques. Double quantum filtered correlation spectroscopy (DQF-COSY),[25] total correlation spectroscopy (TOCSY),[26] and nuclear Overhauser enhancement spectroscopy (NOESY)[27] experiments were recorded on a Bruker 600 MHz. To check the absence of an aggregation state of the peptides, spectra were acquired in the concentration range of 0.2–5 mM. No significant changes were observed in the distribution and in the shape of the ^1H resonances, indicating that no aggregation phenomena occurred in this concentration range. Almost complete ^1H chemical shift assignments for the three analyzed peptides were effectively achieved (Supplementary material). Interchain nuclear Overhauser effect (NOE) between $C^{\beta}H$'s of Cys^5 and Cys^{10}, between $N^{\gamma}H$ of Dap^5 and $C^{\beta\gamma}H$'s of Glu^{10} and between $N^{\varepsilon}H$ of Orn^5 and $C^{\beta}H$'s of Asp^{10} confirmed the presence of the disulfide in hU-II and of the lactam bridges in **2** and **3**, respectively. The preferred conformations of peptides hU-II, **2**, and **3** were derived from the analysis of NMR derived experimental data (NOEs, $^3J_{H\alpha-HN}$ coupling constants, and temperature coefficients of amide protons; see Fig. 2).

Solution conformations of hU-II. Diagnostic NOEs between $C^{\alpha}H$ of Thr^2 and $C^{\delta}H$'s of Pro^3 established a *trans* conformation for the Pro^3 amide bond. From the NOESY spectra, Val^{11} amide proton signal was not observed, probably due to chemical exchange. A qualitative evaluation of the NOE connectivities (Fig. 2) showed no evidence for ordered α-helix or β-sheet structures. $C^{\alpha}H$–HN (i, $i+2$) NOE interactions observed between residues Thr^2-Asp^4, Pro^3-Cys^5, Asp^4-Phe^6, and Lys^8-Cys^{10} indicate the presence of turns along these positions. The observed values of the temperature coefficients of the amide protons (Fig. 2) indicate that all the NHs are solvent exposed, with the exception of the NH of Trp^7. $^3J_{H\alpha-HN}$ coupling constants (Fig. 2) were less informative, with all values falling between 5 and 8 Hz. NMR derived constraints for hU-II (Table 3) were used as input data for a torsion angle dynamics structure calculation as implemented in the DYANA program.[28] NOEs were translated into interproton distances and used as constraints in subsequent annealing procedures to produce 200 conformations. The 50 structures whose interproton distances best fitted NOE derived distances for both groups of 200 initial structures were then refined through successive steps of unrestrained energy minimization (EM) calculations using the program Discover (Biosym, San Diego, USA). A family of 20 structures satisfying the NMR derived constraints (violations smaller than 0.5 Å) was chosen for further analysis (Fig. 3). The PROMOTIF program, was used to extract details of the location and types of structural secondary motifs.[29] As expected from previously published urotensin NMR structures,[15b,30] the hexacyclic region of hU-II was well defined possessing an average root mean square (RMS) deviation of the backbone heavy atoms equal to 0.47 Å (Fig. 3, and Table 4). Side-chain orientations of the residues belonging to this region were also sufficiently defined (the average RMS deviation for all non-hydrogen atoms was 1.36 Å). The residues located

Table 2. Analytical data for the U-II analogues synthesized in this study

Peptide	Structure	HPLC [a]	FAB-MS (M + H)	
		k'	Found	Calcd
1	H-Asp-c[Dap-Phe-Trp-Lys-Tyr-Asp]-Val-OH	7.88	1040.30	1040.26
2	H-Asp-c[Dap-Phe-Trp-Lys-Tyr-Glu]-Val-OH	8.06	1055.50	1055.45
3	H-Asp-c[Orn-Phe-Trp-Lys-Tyr-Asp]-Val-OH	8.28	1068.30	1068.22
4	H-Asp-c[Lys-Phe-Trp-Lys-Tyr-Asp]-Val-OH	7.45	1082.30	1082.24
5	H-Asp-c[Lys-Phe-Trp-Lys-Tyr-Glu]-Val-OH	7.68	1095.60	1095.55

[a]HPLC was performed on an analytical C_{18} column (Vydac 218TP104) using a gradient of CH_3CN in 0.1% aqueous TFA 10–90% in 45 min at a flow rate of 1.0 mL/min; $k' = [(\text{peptide retention time} - \text{solvent retention time})/\text{solvent retention time}]$.

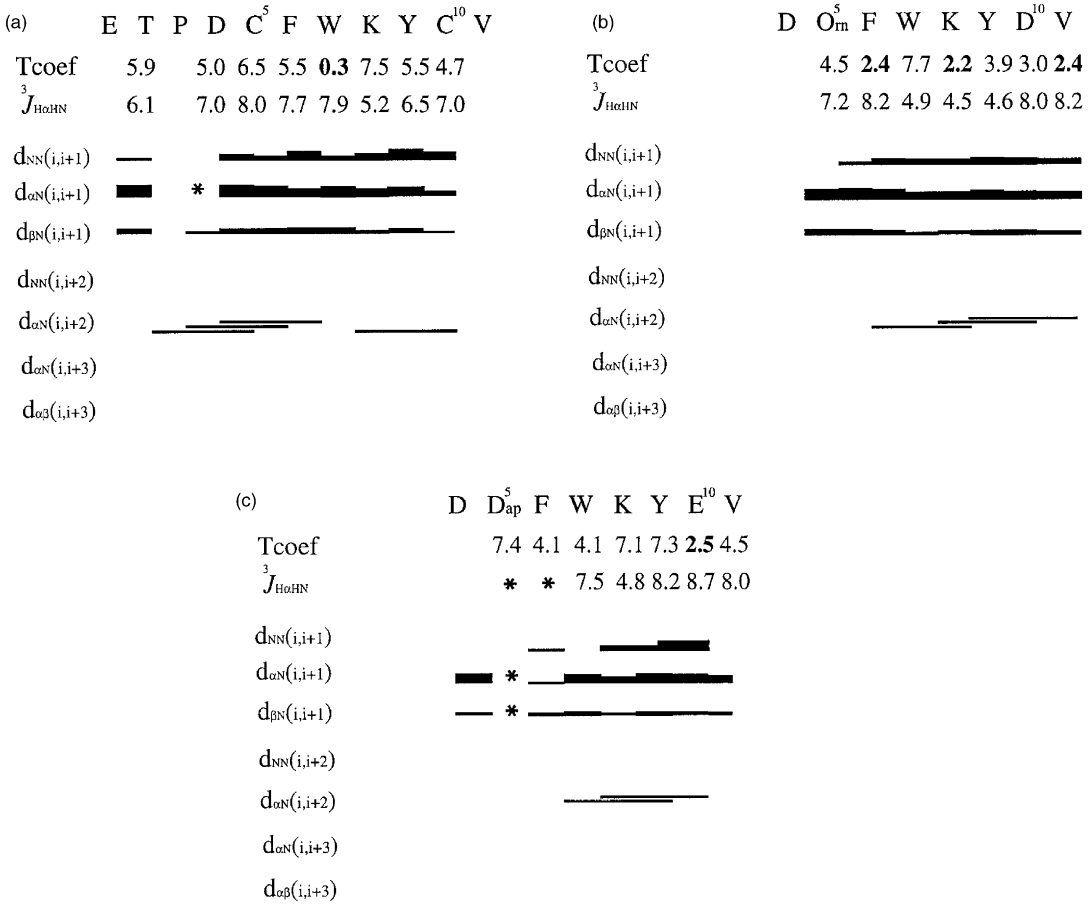

Figure 2. Summary of NMR derived experimental data of peptides hU-II (a), **3** (b), and **2** (c). Temperature coefficients ($-\Delta\delta/\Delta T$) of the amide protons are listed in ppb/K. They are the results of a linear regression analysis of the chemical shifts measured in the range 300–320 K and accurate to within ± 0.4 ppb/K. $^{3}J_{H\alpha-HN}$ coupling constants (Hz) are derived from DQF-COSY spectra analysis.[26] Schematic bar diagrams show the NOE connectivities observed in the NOESY spectra. Thickness of the bars is related to the NOE intensities.

Table 3. NOEs used as restraints in SA calculation

Peptide	Intraresidual	Sequential	Medium range	Total
hU-II	35	64	17	116
2	32	28	16	76
3	37	52	12	101

outside the cycle were less defined (overall backbone heavy atoms RMS deviation = 1.66 Å) indicating higher conformational freedom for these residues. Nevertheless, a type I β-turn was observed in 13 out of 20 calculated structures about residues Thr[2]-Pro[3]-Asp[4]-Cys[5]. This structural element may possibly be relevant for the hU-II activity since it has been reported that the cyclic portion represents the biologically active fragment.[3,17] In spite of the excellent structural definition of the cyclic region, no standard pattern of secondary structures was observed. This is in line with previous NMR studies on teleostean fish U-II,[30] and on hU-II.[15b] The calculated structures showed that aromatic residues Phe[6], Trp[7], and Tyr[9] of the core region project toward one side of the molecule, with respect to the pseudo-plane defined by the cyclic atoms, forming a cluster (Fig. 3), while Lys[8] projects in a direction approximately perpendicular to that of the aromatic residues.

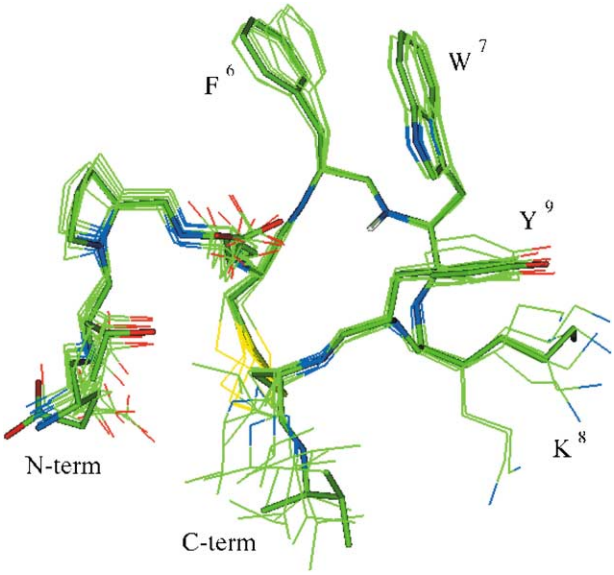

Figure 3. Superposition of the best 10 structures of hU-II. Heavy atoms are shown with different colours (carbon, green; nitrogen, blue; oxygen, red; sulphur, yellow). The most representative structure (i.e., the most similar to the mean structure) is shown with ticker sticks. Amide proton of Trp[7] is also shown (light gray). Backbone carbonyl oxygen atoms are not shown for clarity.

Table 4. Statistical data for hU-II, **2**, and **3** structures

Peptide	Residues	Avg backbone RMSD (Å)	Avg all heavy RMSD (Å)	Violations (Å)
hU-II	5–10	0.47	1.36	<0.5
2	5–10	0.30	0.82	<0.4
3	5–10	0.37	0.59	<0.5

In the calculated structures the amide proton of Trp^7 does not result to be engaged in any hydrogen bond. The low value of the temperature coefficient (−0.3 ppb/K) of this proton derives from its spatial location. In fact, it lies deeply buried into the cluster of the aromatic side chains which protects it from solvent exposure (Fig. 3).

Solution conformations of peptide 3. A qualitative evaluation of the NOE connectivities observed in the NOESY spectra of **3** showed no evidence for α-helix or β-sheet structures. $C^{\alpha}H$–HN (i, $i+2$) dipolar couplings observed between residues Phe^6-Lys^8, Lys^8-Asp^{10}, and Tyr^9-Val^{11} indicate the presence of turns along these positions (Fig. 2). Low values of temperature coefficients ($|\Delta\delta/\Delta T| < 3$ ppb/K) observed for amide protons of residues Phe^6, Lys^8, and Val^{11} together with low values of $^3J_{H\alpha-HN}$ coupling constants ($^3J_{H\alpha-HN} < 5.0$ Hz) observed for residues Trp^7, Lys^8, and Tyr^9 support this hypothesis. Structure calculations were performed as described above. Figure. 4 shows the calculated structures of peptide **3**. The cyclic region appeared to be very well defined with an average RMS deviation of 0.30 and 0.82 Å for the backbone heavy atoms and all non-hydrogen cyclic atoms, respectively. The N- and C-terminal residues of the peptide (Asp^4 and Val^{11}, respectively) were less defined (the average RMS deviation for all non-hydrogen atoms of the molecule increased to 1.50 Å). Secondary structure evaluation of the calculated conformations shows the presence of the following structural motifs: (a) an inverse γ-turn about Asp^4-Orn^5-Phe^6 residues, stabilized by a H-bond between the carbonyl oxygen of Asp^4 and the backbone amide proton of Phe^6 in 12/20 structures; (b) a classic γ-turn about Phe^6-Trp^7-Lys^8 residues, stabilized by a H-bond between the carbonyl oxygen of Phe^6 and the backbone amide proton of Lys^8 in all the calculated structures; (c) β-turns of different types about Lys^8-Tyr^9-Asp^{10}-Val^{11} residues (type I, type VIII, and type IV found in 3/20, 4/20 and 12/20 structures, respectively), stabilized by a H-bond between the carbonyl oxygen of Lys^8 and the backbone amide proton of Val^{11}. These structural motifs are fully consistent with the experimental data. Regarding the side-chain orientations of the cyclic not bridged residues of **3**, Phe^6 and Tyr^9 project toward one side of the molecule and Lys^8 lies approximately in a perpendicular direction (Fig. 4). The presence of the classic γ-turn along residues 6–8 forces the Trp^7 side chain to be oriented on the opposite side of the molecule relative to the other two aromatic side chains.

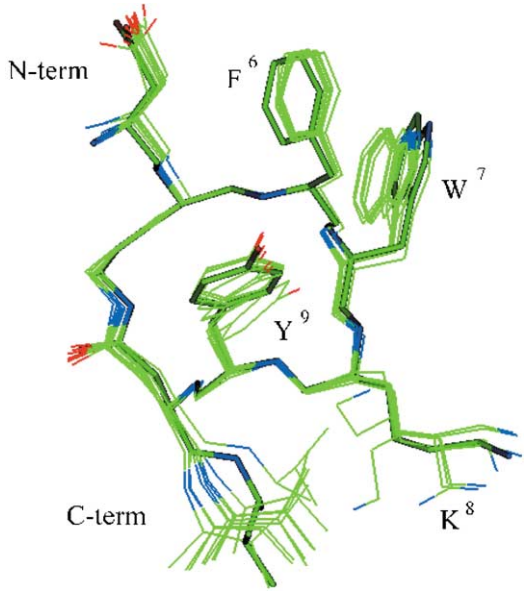

Figure 4. Superposition of the best 10 structures of peptide **3**. Heavy atoms are shown with different colours (carbon, green; nitrogen, blue; oxygen, red). The most representative structure (i.e., the most similar to the mean structure) is shown with ticker sticks. Backbone carbonyl oxygen atoms are not shown for clarity.

Solution conformations of peptide 2. A qualitative evaluation of the NOE connectivities observed in the NOESY spectra of **2** showed no evidence for α-helix or β-sheet. $C^{\alpha}H$–HN (i, $i+2$) dipolar couplings observed between residues Trp^7-Tyr^9, and Lys^8-Glu^{10} along with relatively strong NOEs between the backbone amide protons of Lys^8 and Tyr^9, Tyr^9 and Glu^{10} indicate the presence of turns along these positions (Fig. 2). Low values of temperature coefficients ($|\Delta\delta/\Delta T| < 3$ ppb) observed for amide protons of residues Glu^{10} and Val^{11} together with low value of $^3J_{H\alpha-HN}$ coupling constant ($^3J_{H\alpha-HN} < 5.0$ Hz) observed for residue Lys^8 support this hypothesis. Structure calculations were performed as described above. Figure. 5 shows the calculated structures of peptide **2**. The backbone atoms of the cyclic region appeared to be very well defined with an average RMS deviation of 0.37 Å (0.59 Å for all backbone heavy atoms). Side chains resulted to be less defined, with an average RMS deviation of 1.26 Å (for all non-hydrogen cyclic atoms). Secondary structure evaluation of the calculated conformations shows the presence of a type I β-turn about Trp^7-Lys^8-Tyr^9-Glu^{10} residues found in all the calculated structures, stabilized by a H-bond between the carbonyl oxygen of Trp^7 and the backbone amide proton of Glu^{10}. Further structural motifs found were: (a) an inverse γ-turn about Asp^4-Dap^5-Phe^6 residues, stabilized by a H-bond between the carbonyl oxygen of Asp^4 and the backbone amide proton of Phe^6 in 15/20 structures; (b) an inverse γ-turn about Dap^5-Phe^6-Trp^7 residues, stabilized by a H-bond between the carbonyl oxygen of Dap^5 and the backbone amide proton of Trp^7 in 11/20 structures; (c) an inverse γ-turn about Tyr^9-Glu^{10}-Val^{11} residues, stabilized by a H-bond between the carbonyl oxygen of Tyr^9 and the backbone amide proton of Val^{11} in 18/20 structures. These structural motifs are fully consistent with the experimental data.

Comparison of the NMR structures of hU-II, 2, and 3. The analysis of the average backbone ϕ and ψ angles of hU-II, **2**, and **3** (Table 5) indicated that the three

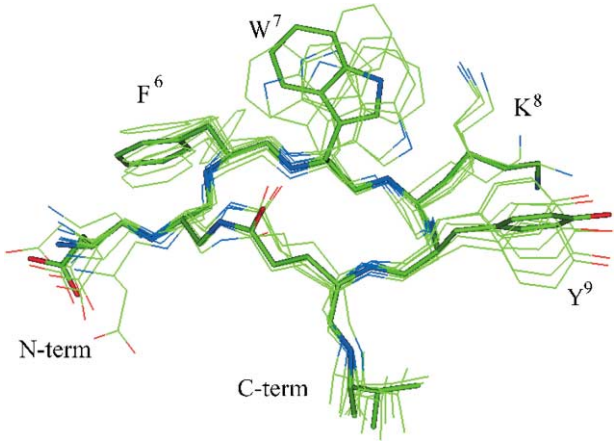

Figure 5. Superposition of the best 10 structures of peptide **2**. Heavy atoms are shown with different colours (carbon, green; nitrogen, blue; oxygen, red). The most representative structure (i.e., the most similar to the mean structure) is shown with ticker sticks. Backbone carbonyl oxygen atoms are not shown for clarity.

Table 5. Values of the ϕ and ψ dihedral angles of residues 5–10 spanning the six-membered cycle of peptides hU-II, **2**, and **3** structures

Angle	hU-II	**2**	**3**
ϕ^5	−74±11	−87±14	−102±28
ψ^5	102±9	90±12	81±13
ϕ^6	−131±28	−87±15	−87±5
ψ^6	−70±3	63±35	75±5
ϕ^7	−125±18	−139±28	70±2
ψ^7	77±21	138±11	−66±7
ϕ^8	50±5	−56±4	−65±9
ψ^8	63±16	−39±7	−31±12
ϕ^9	−142±8	−78±44	−59±10
ψ^9	−43±20	0±23	−48±5
ϕ^{10}	−100±35	−87±23	−90±7
ψ^{10}	−146±89	89±26	23±62

peptides populate different conformational spaces. Nevertheless, the structures of hU-II and peptide **3** can be efficiently superimposed by fitting of heavy atoms of Phe[6], Lys[8], and Tyr[9] residues (Fig. 6). Actually, the side chains of Phe[6], Lys[8] and Tyr[9] adopt a similar spatial arrangement showing a RMS deviation of 1.3 Å. On the contrary, the side chains of Trp[7] point in opposite directions for the two peptides and could not be superimposed. Finally, no efficient way to superimpose peptide **2** calculated structures with those of either hU-II or peptide **3** could be found.

Discussion

The aim of the present study was the design of a synthetic analogue of hU-II in which the disulfide bridge was replaced by a chemically more stable moiety. The importance of the U-II cyclic structure was previously shown by McMaster et al.,[17] who reported a lack of biological activity for the corresponding 'ring-opened' *S*-carboxymethylated analogue. Accordingly, lactam bridges of different lengths were introduced to replace the disulfide bridge in the minimum active fragment of hU-II, that is hU-II(4–11).[3,17] The length of the lactam bridge was continuously modulated between 20 and 24

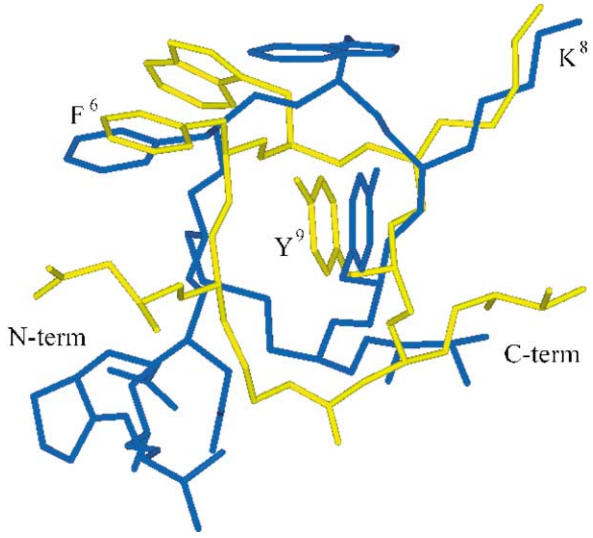

Figure 6. Superposition of the most representative structure of hU-II (blue), with the corresponding one of peptide **3** (yellow). Structures were superimposed by fitting heavy atoms of residues Phe[6], Lys[8], Tyr[9].

atoms. From a formal approach, the smallest ring-containing sequence (analogue **1**) has the same length as the native peptide containing the two Cys residues. Interestingly, the pharmacological data reported in Table 1 indicates that **1** was virtually inactive. In contrast, peptide **3**, characterized by a larger ring (Asp-Orn; 22 atoms), behaved as a full agonist, but was approximately 100-fold less potent than hU-II. The three other analogues with ring sizes containing 21, 23, and 24 atoms were all inactive both as agonists and antagonists.

Several examples of a successful replacement of a disulfide to a lactam bridge have been reported in the literature. For example, two different family members of conotoxins, neurotoxins characterized by two disulfides, were subjected to the disulfide–lactam exchange. For both (des-Glu[1]) conotoxin GI[18a] and α-conotoxin SI,[18b] the replacement of the larger disulfide bridge (positions 3–13) by a Asp-Dap or Glu-Lys lactam, respectively, yielded active analogues. However, in both cases the smaller ring (positions 2–7) did not tolerate the same substitution. In the biologically related peptide endothelin-1, the replacement of the outer disulfide (positions 1–15) by a Dap-Asp lactam gave rise to an antagonist.[19] Thurieau et al.[21] reported the replacement of the disulfide bridge of a somatostatin analogue, angiopeptin (H-DNal-Cys-Tyr-DTrp-Lys-Val-Cys-Thr-NH_2), by lactam bridges of different size. This study was particularly relevant to our research since U-II is structurally and biologically related to somatostatin[8a] as well as the angiopeptin analogue is highly homologous to hU-II(4–11). These authors prepared three angiopeptin lactam analogues, containing ring sizes of 20, 22, and 24 atoms (Asp-Dap, Glu-Dab, and Glu-Lys, respectively). Interestingly, only the Glu-Dab peptide (22 atom ring size) maintained comparable affinity and potency for somatostatin receptors compared to the unmodified peptide. These results agree with those of the present study that the only hU-II lactam analogue maintaining

full agonist activity was characterized by a ring size of 22 atoms (Orn-Asp bridge).

Peptide analogues in which the lactam is introduced as a conformational constraint and not as a disulfide mimetic further demonstrates that the size of the lactam bridge is a crucial parameter which can drastically affect the biological activity. The ring size of the lactam bridged, constrained analogues of both dynorphin A[31] and calcitonin[32] have shown to influence the biological activity as it relates to potency or receptor subtype selectivity. Another relevant example in the field of vasoactive peptides is angiotensin II: a number of constrained, cyclic analogues of this peptide, stabilized by either lactam or disulfide bonds, have been synthesized. Conformational studies of these analogues led to the development of a 3-D model and to the subsequent design of new, more potent peptides.[33]

Finally, the conformational preference in solution of peptides **2** and **3** were compared to hU-II. The structure of the cyclic portion of U-II was well defined, and the side chains of the aromatic residues reported to be important for biological activity[15] appeared to be close to each other, forming a cluster (Fig. 3). The lactam analogues **2** and **3** also displayed a very well defined solution structure (Figs 4 and 5). A superposition of the structures of hU-II and **3** (Fig. 6) clearly indicated that three out of the four key residues (i.e., Phe^6, Lys^8 and Tyr^9) maintained the same side– chain orientation and spatial position, while Trp^7 could not be superimposed. On the contrary, any attempt to superimpose the inactive analogue **2** was unsuccessful. Recent SAR studies on hU-II indicated that the side– chains of residues Trp^7, Lys^8, and Tyr^9 are essential for biological activity.[15] In accordance with these findings, two of these side chains in the active compound **3** can be efficiently superimposed to the corresponding ones of hU-II. The observed reduced activity of **3**, as compared to hU-II, is probably due to the different orientation of Trp^7 side–chain. However, in the above mentioned work[15] the inversion of the configuration of Trp^7 residue appears to be tolerated in the receptor binding assay.

To conclude, we have shown that replacement of the disulfide bridge by a lactam bridge of appropriate length in the cyclic portion of hU-II maintained the bioactivity, thus demonstrating that the disulfide bridge of U-II is not essential for biological activity. The partial loss of activity observed in the synthetic analogue **3**, as compared to the native peptide, appears to be due to the different orientation of one of the key amino acid side chains.

Experimental

Synthesis

Materials. N^{α}-Fmoc-protected amino acids, HBTU and HOBt were purchased from Inbios (Naples, Italy). Wang resin was purchased from Advanced ChemTech (Louisville, KY, USA). N^{α}-Fmoc-amino acids protected as Allyl and Alloc groups were purchased from Neosystem (Strasbourg, France). All protected amino acid derivatives were analyzed for purity by thin-layer chromatography prior to use. Peptide synthesis solvents, reagents, as well as CH_3CN for HPLC were reagent grade and were acquired from commercial sources and used without further purification unless otherwise noted. TLC was performed on Analtech, Inc. (Newark, DE, USA) silica gel 60 F_{254} plates using the following solvent systems: (A) 1-butanol/acetic acid/pyridine/water (5:5:1:4); (B) ethyl acetate/pyridine/acetic acid/water (5:5:1:3); (C) upper phase of 1-butanol/acetic acid/water (4:1:1). The peptides were detected on the TLC plates using iodine vapor.

The synthesis of hU-II lactam analogues was performed manually, utilizing an N^{α}-Fmoc strategy recently developed in our laboratory.[22] N^{α}-Fmoc-Val-OH was coupled to Wang resin (0.5 g, 0.7 mmol NH_2/g). The following protected amino acids were then added stepwise N^{α}-Fmoc-Yaa(Allyl)-OH (Yaa: Asp or Glu, see Table 1), N^{α}-Fmoc-Tyr(O*tert*-butyl (*t*Bu))-OH, N^{α}-Fmoc-Lys(N^{ε}-*tert*-butyloxycarbonyl (Boc))-OH, N^{α}-Fmoc-Trp(N^{in}-Boc)-OH, N^{α}-Fmoc-Phe-OH, N^{α}-Fmoc-Xaa(Aloc)-OH (Xaa: Dap, Orn or Lys) and N^{α}-Fmoc-Asp(O*t*Bu)-OH. Each coupling reaction was accomplished using a 3-fold excess of amino acid with HBTU, HOBt, and DIPEA (6:6:12 equiv). The N^{α}-Fmoc protecting groups were removed by treating the protected peptide resin with a 25% solution of piperidine in *N,N*-dimethylformamide (DMF) , (1×5 and 1×20 min). The peptide resin was washed three times with DMF and the next coupling step was initiated in a stepwise manner. All reactions were performed under an Ar atmosphere. Following linear assembly of the protected peptide resin, the N^{γ}-Alloc and the Allyl groups were removed according to the following procedure: 500 mg of peptide resin was washed with dichloromethane (DCM) under Ar and a solution of $PhSiH_3$ (24 equiv) in 2 mL of DCM was added. Subsequently a solution of $Pd(PPh_3)_4$ (0.25 equiv) in 6 mL of DCM was added and the reaction was allowed to proceed under Ar for 30 min. The peptide resin was washed with DCM (3×), DMF (3×) and DCM (4×), and the deprotection protocol was repeated. The macrocyclic lactam ring formation was mediated by addition of HBTU (6 equiv), HOBt (6 equiv) and DIPEA (12 equiv) for 2 h. The process was repeated if necessary (Kaiser test used to monitor completion).[34] The N-terminal Fmoc group was removed as described above and the peptide was released from the resin with $TFA/Et_3SiH/H_2O$ (90:5:5) for 3 h.[22] The resin was removed by filtration and the crude peptide was recovered by precipitation with cold anhydrous ethyl ether to give a white powder which was purified by RP-HPLC on a semi-preparative C18-bonded silica column (Vydac 218TPP1010, 1.0 × 25 cm) using a gradient of CH_3CN in 0.1% aqueous TFA (from 10 to 90% in 45 min) at a flow rate of 1.0 mL/min. The product was obtained by lyophilization of the appropriate fractions after removal of the CH_3CN by rotary evaporation. Analytical RP-HPLC indicated a purity >98% and molecular weights were confirmed by fast-atom bombardment mass spectrometry (FAB-MS) (Fisons

mod. Prospec) or high resolution mass spectrometry (HR-MS) (Kratos Analytical mod. Kompact) (see Table 2).

Pharmacology

Male albino rats (Wistar strain, 300–350 g) were stunned and bled. The thoracic aorta was cleared of surrounding tissue and excised from the aortic arch to the diaphragm. The vessel was opened along the longitudinal axis and the endothelium removed by gently rubbing its intimal surface with a cotton-tip applicator. The effectiveness of this maneuver was assessed by the loss of relaxation response to acetylcholine (1 μM) in noradrenaline (1 μM)-precontracted preparations. From each aorta, a helically-cut strip was prepared that was subsequently divided into two parallel strips. All preparations were placed in 5– mL organ baths filled with oxygenated (96% O_2 and 4% CO_2) Krebs–Henseleit solution with the following composition: NaCl, 119 mM; $NaHCO_3$, 25 mM; KH_2PO_4, 1.2 mM; $MgSO_4$, 1.5 mM; $CaCl_2$, 2.5 mM; KCl, 4.7 mM and glucose 11 mM. The motor activity of aortic strips was recorded isotonically (load 5 mN). Cumulative concentration-response curves to hU-II and the cyclic lactam analogues were constructed, each concentration being added when the effect of the preceding one had reached a steady state. Maximal contractile responses of preparations were induced by administration of KCl (80 mM). Agonist activity of all compounds was expressed as pD_2 ($-\log EC_{50}$; EC_{50}: molar concentration of peptide producing 50% of maximal effect); each reported value is the mean ± SEM of at least four determinations.

Conformational studies

Sample preparation. DMSO-d_6 was obtained from Aldrich (Milwaukee, USA). The samples for NMR spectroscopy were prepared by dissolving the appropriate amount of hU-II, **2** and **3** in 0.5 mL DMSO-d_6 (99.96%) to obtain a 4 mM concentration.

NMR experiments. NMR spectra were recorded on a Bruker DRX-600 spectrometer. All the spectra were recorded at a temperature of 300 K, except for the temperature coefficients, which were measured for the amide proton resonances by variation of the temperature from 300 to 320 K. One-dimensional (1D) NMR spectra were recorded in the Fourier mode with quadrature detection and the water signal was suppressed by a low-power selective irradiation in the homogated mode. 2D DQF-COSY,[25] TOCSY[26] and NOESY[27] experiments were run in the phase-sensitive mode using quadrature detection in ω_1 by time-proportional phase increase of initial pulse.[35] Data block sizes were 4096 addresses in t_2 and 512 equidistant t_1 values. Before Fourier transformation, the time domain data matrices were multiplied by shifted $\sin^2$ functions in both dimensions. A mixing time of 70 ms was used for the TOCSY experiments. NOESY experiments were run at 300 K with mixing times in the range of 150–300 ms. The spectra were calibrated relative to DMSO-d_6 (2.50 ppm) as internal standard. The qualitative and quantitative analyses of DQF-COSY, TOCSY, and NOESY spectra, were obtained using the interactive program package XEASY.[36]

Structural determinations and computational modeling. The NOE-based distance restraints were obtained from NOESY spectra collected with a mixing time of 200 ms. The NOE cross peaks were integrated with the XEASY program and were converted into upper distance bounds using the CALIBA program incorporated into the program package DYANA.[28] Cross peaks which were overlapped more than 50% were treated as weak restraints in the DYANA calculation. An ensemble of 200 structures was generated with the program DYANA using 99 (intraresidue and sequential) and 17 (medium range) NOE-based distance constraints for hU-II, 60 (intraresidue and sequential) and 16 (medium range) for peptide **2**, and 89 (intraresidue and sequential) and 12 (medium range) for peptide **3**. The 50 structures with the lowest value of the target function from the DYANA-generated sets for both peptides were subjected to extensive minimization. Steepest descents minimizations without distance restraints were performed on all structures with the Discover 2.9 algorithm (Biosym, San Diego, USA) utilizing the consistent valence force field (CVFF).[37] Minimization proceeded until the change in energy was less than 0.05 kcal/mol. This was followed by conjugate gradient energy minimization until the change in energy was less than 0.01 kcal/mol. A distance-dependent dielectric constant equal to r was applied to evaluate electrostatic interactions. The minimization lowered the total energy of the structures; no residue was found in the disallowed region of the Ramachandran plot. The final structures were analyzed using the Insight 95.0 program (Biosym, San Diego, USA). Graphical representation and RMS deviation analysis between energy minimized structures were carried out with the programs MOLMOL,[38] and INSIGHTII (Biosym, San Diego, USA).

References and Notes

1. Pearson, D.; Shively, J. E.; Clark, B. R.; Geschwind, I. I.; Barkley, M.; Nishioka, R. S.; Bern, H. A. *Proc. Natl. Acad. Sci. U.S.A.* **1980**, *77*, 5021.
2. Bern, H. A.; Pearson, D.; Larson, B. A.; Nishioka, R. S. *Recent Progr. Horm. Res.* **1995**, *41*, 533.
3. Itoh, H.; Itoh, Y.; Rivier, J.; Lederis, K. *Am. J. Physiol.* **1987**, *252*, R361.
4. Coulouarn, Y.; Lihrmann, I.; Jegou, S.; Anouar, Y.; Tostivint, H.; Beauvillain, J. C.; Conlon, J. M.; Bern, H. A.; Vaudry, H. *Proc. Natl. Acad. Sci. U.S.A.* **1998**, *95*, 15803.
5. Ames, R. S.; Sarau, H. M.; Chambers, J. K.; Willette, R. N.; Aiyar, R. V.; Romanic, A. M.; Louden, C. S.; Foley, J. J.; Sauermelch, C. F.; Coatney, R. W.; Ao, Z.; Disa, J.; Holmes, S. D.; Stadel, J. M.; Martin, J. D.; Liu, W.-S.; Glover, G. I.; Wilson, S.; McNutty, D. E.; Ellis, C. E.; Eishourbagy, N. A.; Shabon, U.; Trill, J. J.; Hay, D. V. P.; Ohlstein, E. H.; Bergsma, D. J.; Douglas, S. A. *Nature* **1999**, *401*, 282.
6. (a) Marchese, A.; Heiber, M.; Nguyen, T.; Heng, H. H.; Saldivia, V. R.; Cheng, R.; Murphy, P. M.; Tsui, L. C.; Shi, X.; Gregor, P.; George, S. R.; O'Dowd, B. F.; Doehrty, J. M. *Genomics* **1995**, *29*, 335—344. (b) Tal, M.; Ammer, D. A.;

Karpuj, M.; Krizhanovsky, V.; Naim, M.; Thompson, D. A. *Biochem. Biophys. Res. Commun.* **1995**, *209*, 752.
7. Libert, F.; Vassart, G.; Parmentier, M. *Curr. Opin. Cell Biol.* **1991**, *8*, 218.
8. (a) Nothacker, H. P.; Wang, Z.; McNeill, A. M.; Saito, Y.; Merten, S.; O'Dowd, B.; Duckles, S. P.; Civelli, O. *Nat. Cell Biol.* **1999**, *1*, 383. (b) Mori, M.; Sugo, T.; Abe, M.; Shimomura, Y.; Kurihara, M.; Kitada, C.; Kikuchi, K.; Shintai, Y.; Kurokawa, T.; Onda, H.; Nishimura, O.; Fujino, M. *Biochem. Biophys. Res. Commun.* **1999**, *265*, 123. (c) Liu, Q.; Pong, S. S.; Zeng, Z.; Zhang, Q.; Howard, A. D.; Williams, D. R.; Davidoff, M.; Wang, R.; Austin, C. P.; McDonald, T. P.; Bai, C.; George, S. R.; Evans, J. F.; Caskey, C. T. *Biochem. Biophys. Res. Commun.* **1999**, *266*, 174.
9. (a) MacLean, M. R.; Alexander, D.; Stirrat, A.; Gallagher, M.; Douglas, S. A.; Ohlstein, E. H.; Morecroft, I.; Polland, K. *Br. J. Pharmacol.* **2000**, *130*, 201. (b) Maguire, J. J.; Kuc, R. E.; Davenport, A. P. *Br. J. Pharmacol.* **2000**, *130*, 441.
10. Douglas, S. A.; Sulpizio, A. C.; Piercy, V.; Sarau, H. M.; Ames, R. S.; Aiyar, N. V.; Ohlstein, E. H.; Willette, R. N. *Br. J. Pharmacol.* **2001**, *131*, 1262.
11. Douglas, S. A.; Ohlstein, E. H. *Trends Cardiovasc. Med.* **2000**, *10*, 229.
12. Hay, D.; Luttmann, M. A.; Douglas, S. A. *Br. J. Pharmacol.* **2000**, *130*, 10.
13. Russel, F. D.; Molenaar, P.; O'Brien, D. M. *Br. J. Pharmacol.* **2001**, *132*, 5.
14. Gardiner, S. M.; March, J. E.; Kemp, P. A.; Davenport, A. P.; Bennett, T. *Br. J. Pharmacol.* **2001**, *132*, 1625.
15. (a) Brkovic, A.; Lampron, F.; Létourneau, M.; Fournier, A. 17th American Peptide Symposium, San Diego, CA, June 9–14, 2001; poster P338. (b) Flohr, S.; Kurz, M.; Kostenis, E.; Brkovich, A.; Fournier, A.; Klabunde, T. *J. Med. Chem.* **2002**, *45*, 1799–1805.
16. Camarda, V.; Rizzi, A.; Calò, G.; Gendron, G.; Perron, S. I.; Kostenis, E.; Zamboni, P.; Mascoli, F.; Regoli, D. *Naunyn-Schmiedeberg's Arch. Pharmacol.* **2002**, *365*, 141.
17. Mc Master, D.; Kobayashi, Y.; Rivier, J.; Lederis, K. *Proc. West. Pharmacol. Soc.* **1986**, *29*, 205.
18. (a) Almquist, G. R.; Kadambi, S. R.; Yasuda, D. M.; Weitl, F. L.; Polgar, W. E.; Toll, L. R. *Int. J. Pept. Protein Res.* **1989**, *34*, 455. (b) Hargittai, B.; Solé, N. A.; Groebe, D. R.; Abramson, S. N.; Barany, G. *J. Med. Chem.* **2000**, *43*, 4787.
19. (a) Spinella, M. J.; Malik, A. B.; Everitt, J.; Andersen, T. T. *Proc. Natl. Acad. Sci. U.S.A.* **1991**, *88*, 7443. (b) Abraham, W. M.; Ahmed, A.; Cortes, A.; Spinella, M. J.; Malik, A. B.; Andersen, T. T. *J. Appl. Physiol.* **1993**, *74*, 2537.
20. Limal, D.; Briand, J.-P.; Dalbon, P.; Jolivet, M. *J. Peptide Res.* **1988**, *52*, 121.
21. Thurieau, C.; Janiak, P.; Krantic, S.; Guyard, C.; Pillon, A.; Kucharczyk, N.; Vilaine, J. P.; Fauchere, J. L. *Eur. J. Med. Chem.* **1995**, *30*, 115.
22. Grieco, P.; Gitu, P. M.; Hruby, V. J. *J. Peptide Res.* **2001**, *57*, 250.
23. Pearson, D. A. *Tetrahedron Lett.* **1989**, *30*, 2739.
24. Amodeo, P.; Motta, A.; Picone, D.; Saviano, G.; Tancredi, T.; Temussi, P. A. *J. Magn. Res.* **1991**, *95*, 201.
25. Piantini, U.; Sorensen, O. W.; Ernst, R. R. *J. Am. Chem. Soc.* **1982**, *104*, 6800.
26. Bax, A.; Davis, D. G. *J. Magn. Reson.* **1985**, *63*, 207.
27. Jenner, J.; Meyer, B. H.; Bachman, P.; Ernst, R. R. *J. Chem. Phys.* **1979**, *71*, 4546.
28. Guntert, P.; Mumenthaler, C.; Wüthrich, K. *J. Mol. Biol.* **1997**, *273*, 283.
29. Hutchinson, E. G.; Thornton, J. M. *Protein Sci.* **1996**, *5*, 212.
30. Bhaskaram, R.; Arunkumar, A. I.; Yu, C. *Biochim. Biophys. Acta* **1994**, *119*, 115.
31. Arttamangkul, S.; Murray, T. F.; DeLander, G. E.; Aldrich, J. V. *J. Med. Chem.* **1995**, *38*, 2410.
32. (a) Kapurniotu, A.; Taylor, J. W. *J. Med. Chem.* **1995**, *38*, 836. (b) Kapurniotu, A.; Kayed, R.; Taylor, J. W.; Voelter, W. *Eur. J. Biochem.* **1999**, *265*, 606.
33. Zhang, W. J.; Nikiforovich, G. V.; Perodin, J.; Richard, D. E.; Escher, E.; Marshall, G. R. *J. Med. Chem.* **1986**, *39*, 2738.
34. Kaiser, E.; Colescott, R. L.; Bossinger, C. D.; Cook, P. I. *Anal. Biochem.* **1970**, *34*, 595.
35. Marion, D.; Wüthrich, K. *Biochem. Biophys. Res. Commun.* **1983**, *113*, 967.
36. Bartels, C.; Xia, T.; Billeter, M.; Guentert, P.; Wüthrich, K. *J. Biomol. NMR* **1995**, *6*, 1.
37. Maple, J.; Dinur, U.; Hagler, A. T. *Proc. Natl. Acad. Sci. U.S.A.* **1988**, *85*, 5350.
38. Koradi, R.; Billeter, M.; Wüthrich, K. *J. Mol. Graph.* **1996**, *14*, 51.